Acta Universitatis Sapientiae
Electrical and Mechanical Engineering, 16 (2024) 38–47

DOI: 10.47745/auseme-2024-0004

Reconstruction of Defect Paths Using Eddy Current Testing Array 3D Imaging

Abderrahmane ABOURA[1], Abdelhak ABDOU[2], Tarik BOUCHALA[3], Mohamed CHEBOUT[4], Bachir ABDELHADI[5], Merwane KHEBAL[6]

[1] Department of Electrical Engineering, Faculty of Science and Technology, University of Msila, e-mail: abderrahmane.aboura@univ-msila.dz (Corresponding Author)
[2] Electrical Engineering Department, Faculty of Science and Technology, University of Batna2, e-mail: abdelhak.abdou@univ-Batna2.dz
[3]Department of Electrical Engineering, Faculty of Science and Technology, University of Msila, e-mail: tarek.bouchala@univ-msila.dz
[4]Department of Electrical Engineering, Faculty of Science and Technology, University of Djelfa, e-mail: m.chebout@univ-djelfa.dz
[5]Department of Electrical Engineering, Faculty of Science and Technology, University of Msila, e-mail: b.abdelhadi@univ-Batna2.dz
[6]Department of Electrical Engineering, Faculty of Science and Technology, University of Msila, e-mail: merwane.khebal@univ-msila.dz

Abstract: In a world where the reliability and lifespan of industrial equipment are critical, our research aims to go beyond the traditional limits of non-destructive testing. We seek to achieve accurate detection and comprehensive imaging of defects in their various forms by harnessing the capabilities of eddy current testing with multiplexing technology on multi-element sensors. This approach allows us to save time and ensure the quality of results. This paper presents a method for detecting and imaging different defect paths on an aluminium plate. Our methodology involves the strategic deployment of multi-sensor techniques specifically designed for eddy current testing. To address the inherent challenge of mutual magnetic induction between these sensors, we employ the alternating feed method, which is an advanced technology that ensures data integrity and significantly accelerates scanning times. By combining this technology with multi-sensor techniques, we capture signals that provide valuable insights into the presence of defects. Additionally, we produce 3D imaging that enables us to trace their paths, regardless of size. These preliminary results lay the foundation for future research aimed at accurately characterizing and visualizing the shapes and dimensions of these defects, thereby contributing to a more comprehensive understanding of defect behaviour.

Keywords: Eddy current testing, multiplexing, eddy current array, imaging defect.

1. Introduction

In the field of non-destructive evaluation (NDE) for conductive materials, eddy current testing (ECT) stands as a leading electromagnetic technique. Grounded in the principles of electromagnetic induction, ECT leverages this phenomenon to deliver its impressive capabilities [1], [2]. When a time-varying magnetic field interacts with a material under examination, it induces eddy currents within the material. Disturbances in these eddy current paths allow for the detection of cracks or other irregularities within the object being inspected. ECT offers a broad range of applications, including material thickness measurements, proximity assessments, corrosion evaluations, and the sorting of materials based on their electromagnetic properties [3].

One of the primary historical applications of ECT was the identification of discontinuities and the subsequent diagnosis of potential issues. In the domains of steam generators and aircraft wing panels for instance [4], [5],[6], stress corrosion cracks (SCC) and fatigue cracks (FC) constitute common forms of structural degradation. However, certain types of defects, such as cavitation and internal corrosion, often elude detection during routine inspections due to their concealed and imperceptible nature [7].

Detection of defects is not always limited to superficial ones, but also to internal and uncovered ones of various sizes [8],[9]. On the other hand, while using a large and representative database, machine learning techniques can evaluate and classify defects according to theirs shape, size and path [10].

In this research endeavor, our focus is centered on employing three-dimensional simulations within the Comsol Multiphysics program [11] to an aluminum plate. The simulations involved the intentional introduction of defects of varying sizes and orientations—namely, straight, zigzag, and circular defects. Subsequently, we analyze the impedance measured by each element of the eddy current sensor array (ECA).

Utilizing this ECA in multiplexed mode enabled the acquisition of 3D imaging, yielding novel and refined results. This approach enhances clarity and precision and paves the way for advanced research opportunities.

By distinctly visualizing and characterizing these defects, we contribute qualitatively to this domain, promoting increased security and safety at a physical level. This is particularly critical in averting potential catastrophic consequences, such as accidents linked to reactors.

Beyond its implications for reactor safety, this research holds significance on a humanitarian level. Emphasizing the importance of reinforcing inspection procedures, our work underscores the crucial role these advancements play in ensuring the safety of both employees and the wider public.

2. Mathematical modeling of the electromagnetic phenomenon

Eddy Current Non-Destructive Testing (ECNDT) is grounded in the principles of electromagnetic fields. The examination and mathematical representation for computing induced currents within the inspected material are based on the laws of electromagnetism, incorporating quasistatic approximations of Maxwell's equations. Various strategies exist for modelling the interaction between the probe and the tested structure, particularly in complex geometries where numerical methods are commonly employed.

The modelling and simulation of eddy current testing provide a robust foundation for an early assessment of part inspection. Numerous numerical formulations, particularly those utilizing the finite element method (FEM), have been proposed to address the challenges associated with this open boundary problem—both in its differential and integral aspects [12]. Noteworthy among the differential formulations are the H-Φ formulation introduced by Bossavit and Verite [13], the T-Ω formulation detailed by Carpenter [14], and later expanded by Brown [15] and Albanese and Rubinacci [16], and the A-V formulation proposed by Biro [17]. The primary advantage of the differential formulation lies in the sparsity of the matrices in the solving system, which is essential for reducing computational costs.

In this manuscript, we employ a three-dimensional Finite Element (FE) methodology to compute signals from eddy current probes in the presence of cracks, with the goal of characterizing material properties. The system of equations governing the dynamics of these multiphysics systems, where variables evolve over time and space, can be derived from Maxwell's equations, as outlined below:

$$\nabla \times (\mu^{-1}\nabla \times \boldsymbol{A}) + j\omega\sigma\boldsymbol{A} + \sigma\nabla V = 0 \quad (1)$$

$$\nabla \cdot \sigma(j\omega\boldsymbol{A} + \nabla V) = 0 \quad (2)$$

$$\nabla \times (\mu^{-1}\nabla \times \boldsymbol{A}) = \boldsymbol{J} \quad (3)$$

$$\boldsymbol{J} = -j\omega\sigma\boldsymbol{A} - \sigma\nabla V \quad (4)$$

Using Galerkin techniques, the imposition of Dirichlet boundary conditions requires fixing nodal potentials at known values [18], [19]. Neumann boundary conditions, on the other hand, are naturally incorporated into the formulation. In our specific scenario, where both the magnetic vector potential and electric scalar potential are utilized, we adopt the Galerkin weak form represented by the following expressions:

$$\int_{\Gamma} \boldsymbol{\Psi} \cdot \nabla \times (\mu^{-1}\nabla \times \boldsymbol{A})d\Gamma + \int_{\Gamma} \sigma\boldsymbol{\Psi} \cdot (j\omega\boldsymbol{A} + \nabla V)d\Gamma = \int_{\Gamma} \boldsymbol{\Psi} \cdot \boldsymbol{J}_s d\Gamma \quad (5)$$

$$\int_{\Gamma} \boldsymbol{\Psi} \cdot \nabla \cdot \sigma(j\omega\,\boldsymbol{A} + \nabla V)d\Gamma = 0 \quad (6)$$

$$Z = R + j\omega L = \frac{1}{I^2}(P + j2\omega W) \quad (7)$$

Γ: The boundary of the domain, often the surface of the material being analyzed, the integrals are computed over this boundary surface.

Ψ: The test (or weight) function used in the weak formulation of the problem; it's used to multiply the terms in the equation to form the weak form of the problem.

The elements of impedance are defined as follows:

$$R = P/I^2 \ , \quad \text{and} \quad L = 2W/I^2 \quad (8)$$

In this instance, the unspecified parameters P and W can be articulated as:

$$P = \int_\Gamma \boldsymbol{J} \cdot \boldsymbol{E}^* \, d\Gamma \text{ and } W = \int_\Gamma \boldsymbol{H} \cdot \boldsymbol{B}^* \, d\Gamma \quad (9)$$

P and W are defined by the specific properties of the material (aluminum) being tested, as their values depend on how the material interacts with electric and magnetic fields. For aluminum, these interactions are influenced by its electrical conductivity and magnetic permeability.

3. Executing and Showcasing the Proposed Models

Having witnessed the impressive effectiveness of COMSOL® Multiphysics simulation software in non-destructive testing using eddy currents in previous work [8], [9], and its consistent delivery of very satisfactory results in line with laboratory-scale experimental results [20], we chose to harness its capabilities in modeling our system, using the AC/DC module.

To streamline the detection of defects and capture their images through meticulous scanning and inspection for path identification, our model employs multiple sensors activated sequentially and alternately, employing a technique known as multiplexing, as illustrated in *Fig. 1*. This method is carefully designed to alleviate potential issues of mutual induction that might arise between adjacent sensors.

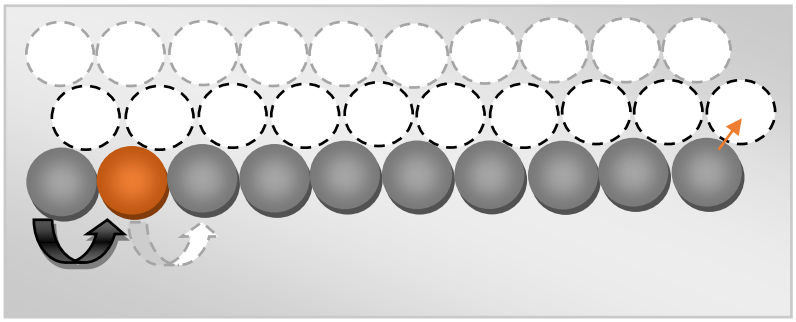

Figure 1: Illustration of the multiplexing method based on eddy current array

Fig. 1 illustrates the sequential activation of individual eddy current coils. The process begins with the orange element being activated, followed by the next element, and so on, until all the sensor elements, depicted in gray, are activated. The sensor then advances in small 1 mm increments, occupying the area shown by the transparent elements (transparent circles) in the figure. This process is repeated until the array of elements covers the entire area to be examined.

This technique, known as multiplexing, essentially combines multiple analog message signals into a unified digital signal on a shared medium. When applied to eddy current array data, multiplexing ensures that no two adjacent elements or coils are activated simultaneously, thereby minimizing the unwanted effects of mutual inductance—magnetic coupling between closely positioned coils. To precisely control each coil when sending its eddy current signal, an internal multiplexing system is employed, which effectively mitigates mutual inductance. The impedances measured by each element of the eddy current array when the probe is moved in the scaning direction, are saved as a matrix in order to be converted to a 3D images under Matlab software.

Beyond enhancing imaging capabilities, multiplexing also allows for post-scan analysis of individual data channels. This approach improves channel resolution, increases sensitivity by reducing mutual inductance, and lowers noise levels, collectively resulting in an improved signal-to-noise ratio.

Each sensor coil has 100 turns of wire with 0.03×10^{-6} m² cross-sectional area and 6×10^{7} S/m conductivity.

The scanning procedure is performed with the probe positioned parallel to the y-axis. The lift-off, which is the distance between the coil and the plate, is set to 0.5 mm.

During the scanning process, each sensor element is advanced step-by-step along the aluminum plate (*Fig. 1*), which has a conductivity of $3.774.10^{7}$ S/m.

The study examines three different defect shapes: C-shape, I-shape, and V-shape. There have been simulated different flaws: straight, inclined, and circular

paths, corresponding to C-shape, I-shape, and V-shape defects as illustrated in the table below and *Fig. 2*, *Fig. 3* and *Fig. 4*.

- **I-Shaped Defect:** This defect consists of two straight segments oriented perpendicularly to each other. Each segment has a length of 20 mm, a width of 1.5 mm, and a depth of 1 mm.
- **V-Shaped Defect:** The V-shaped defect is composed of two equal sides, each measuring 15 mm in length, forming a symmetrical configuration. The vertex of the V-shape includes a convex arc with an outer radius of 2 mm and an inner radius of 1 mm. Both the width and depth of this defect measure 1 mm.
- **C-Shaped Defect:** The C-shaped defect is a semicircle with an outer radius of 17 mm and an inner radius of 15 mm. The width, calculated as the difference between the outer and inner radii, is 2 mm. The depth of the defect is also 2 mm.

Table 1: Parameter values

Plate parameter value [mm]	Plate width 100	Plate length 100	Plate thickness 8
Defect_I-shape parameter value[mm]	Crack width 1	Crack length 20	Crack depth 1
Defect_V-shape parameter value[mm]	Crack width 1	Crack length 30	Crack depth 1
Defect_C-shape parameter value [mm]	Crack width 2	Crack length 47.1-53.4	Crack depth 2
Sensor parameter value [mm]	Coil inner 0.5	Coil outer 2	Coil height 2
Physical parameter value	Relative Permeability 1	Frequency 10000 Hz	Lift-off 0.5 mm

The type of element used significantly impacts the number of degrees of freedom required for the numerical resolution of the problem. In our study, we opted for tetrahedral elements in our mesh, as this choice facilitates automatic meshing of various geometries.

The selection of element size greatly influences the accuracy of the numerical solution obtained. To accurately capture the variations in the quantities of interest, it's crucial to tailor the mesh size to the specific problem at hand. Balancing mesh sizes across different domains is illustrated in (*Fig. 2*).

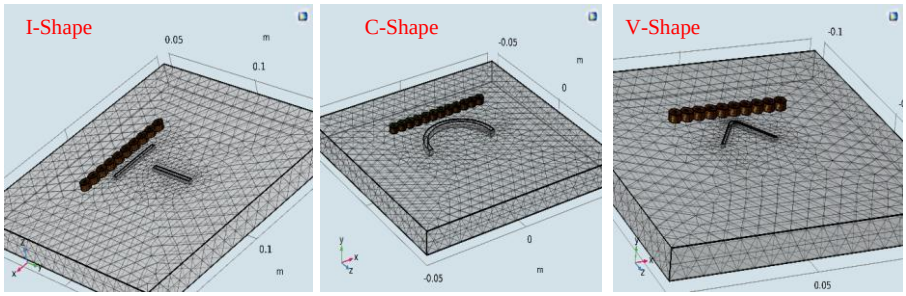

Figure 2: Geometry and meshing for different defect shapes

4. Reconstruction of defect shape from the impedance amplitude impedance

Fistly, we move the eddy cuurent array (ECA) sensor according to the appropriate axis and we record the obtained impedance and position of each element. Then, we reconstruct the carthography of the impedance on the scanned surface for different defect shapes (I, C and V shapes). In fact, the obtained results are shown in *Fig. 3*.

Upon analyzing the results obtained in all three cases, it is evident that the defect has been successfully reconstructed with its true shape and trajectory. As a result, the diagnosis of the defect has become not only faster but also more accurate and reliable. However, for a more comprehensive assessment of the defect, it is crucial to determine its unknown depth. This aspect can be addressed in future work by utilizing techniques such as neural networks or other probabilistic and deterministic methods to extract and track the defect depth through the impedance measurements in the affected area.

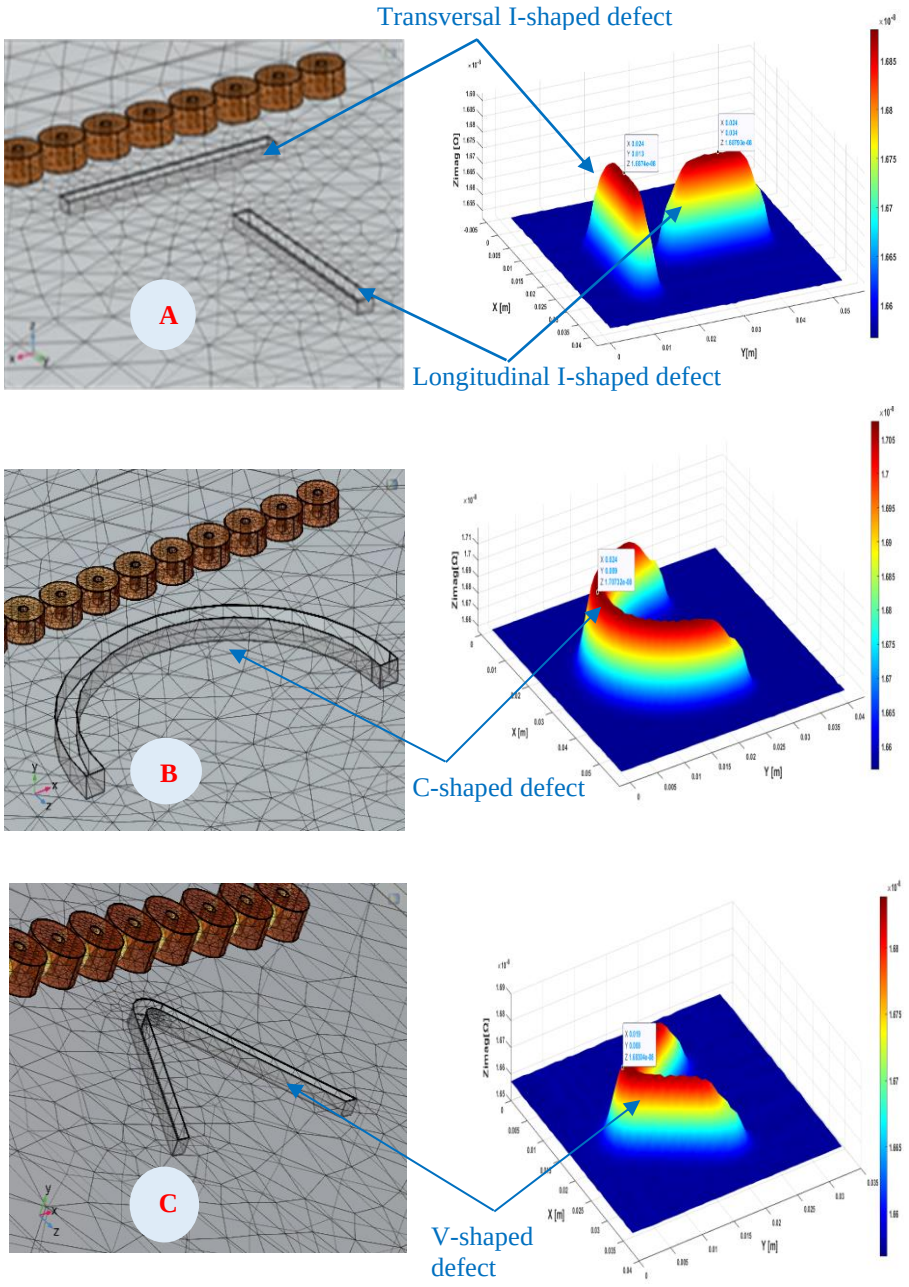

Figure 3: Defect shape reconstruction from impedance amplitude imaging for three cases. A, B and C represent I, C and V defect shapes, respectively

5. Conclusion

In this study, we introduced a model designed to detect defects of varying sizes along diverse paths and orientations, including straight, inclined, and circular trajectories. Our approach employed multiplexing technology operating at a fixed frequency in harmonic mode.

Utilizing ECA probe, impedance data were gathered at each position, leveraging the multiplexing method to mitigate mutual induction between sensing elements and simplifying the exciting electric circuit. This enabled efficient detection of surface defects and subsequent determination of their paths through 3D imaging, achieved by organizing impedance data in alignment with the sensors' scanning path.

The obtained results underscore the significance of this technique, streamlining the detection process and providing comprehensive defect images. Further research is anticipated to enhance our understanding and provide a more comprehensive depiction of defect dimensions.

For future work, this study can be expanded by incorporating additional important parameters. One key aspect to explore is defect depth estimation, as it is a critical factor in nondestructive testing applications due to the potential severity of deep defects. Additionally, since defect depth often varies in practice, investigating defects with irregular depth would provide valuable insights. The advancement of artificial intelligence (AI) could also be leveraged to identify, classify, and characterize complex defects, particularly when utilizing a comprehensive and well-structured database.

References

[1] Ruzlaini, G., Mahmood, D., Aizat, S., & Mamat, I. F., "Defect Characterization Based on Eddy Current Technique: Technical Review," *Advances in Mechanical Engineering*, 6, 1–11, 2014. https://doi.org/10.1155/2014/182496.

[2] Kot, P., Muradov, M., Gkantou, M., Kamaris, G. S., Hashim, K., & Yeboah, D., "Recent advancements in non-destructive testing techniques for structural health monitoring," *Applied Sciences*, 11(6), 2750, 2021. https://doi.org/10.3390/app11062750.

[3] Wen, D., Fan, M., Cao, B., & Ye, B., "Adjusting LOI for Enhancement of Pulsed Eddy Current Thickness Measurement," *IEEE Transactions on Instrumentation and Measurement*, 69(2), 521–527, 2020. https://doi.org/10.1109/TIM.2019.2904331.

[4] Stolyarova, A. A., Lunina, V. P., Zhdanova, A. G., & Shchukisa, E. G., "Revealing and Assessing the Deposit Amount on Heat-Exchanger Tubes of NPP Steam Generators According to the Operational Data of Routine Eddy Current Monitoring," *Thermal Engineering*, 67(2), 129–137, 2020. https://doi.org/10.1134/S0040601519120103.

[5] Yang, G., Dib, G., Udpa, L., Tamburrino, A., & Udpa, S. S., "Rotating field EC-GMR sensor for crack detection at fastener site in layered structures," *IEEE Sensors Journal*, 15(1), 463–470, 2015. https://doi.org/10.1109/JSEN.2014.2341653.

[6] Valentyn, V., "Enhanced eddy current techniques for detection of surface-breaking cracks in aircraft structures," *Transport and Aerospace Research*, 2021(1), 1–14, 2021. https://doi.org/10.2478/tar-2021-0001.
[7] Wang, L., & Chen, Z., "Sizing of crack using multi-output support vector regression method from multi-frequency eddy current testing signals," *International Journal of Applied Electromagnetics and Mechanics*, 64(1–4), 721–728, 2020. https://doi.org/10.3233/JAE-209383.
[8] Abderrahmane, A., Abdelhak, A., Bouchaala, B., Abdeslam, A., & Merwane, K., "Scanning by multi-sensors to detect surface and internal defects," *Proceedings of the 2022 International Conference of Advanced Technology in Electronic and Electrical Engineering (ICATEEE)*, 2022. https://doi.org/10.1109/ICATEEE57445.2022.10093732.
[9] Aboura, A., Abdou, A., Bouchala, T., Khebal, M., Abdelhadi, B., & Guettafi, A., "Inspection of aluminum sheets using a multi-element eddy current sensor: 2D and 3D imaging of surface defects of various sizes and internal defects at various depths," *Studies in Engineering and Exact Sciences*, 5(2), e5786, 2024. https://doi.org/10.54021/seesv5n2-024.
[10] Bangda, C., Zhijie, Z., Yuliang, W., Dong, W., & Zexue, Z., "A metal classification system based on eddy current testing and deep learning," *IEEE Sensors Journal*, 24(3), 3266–3276, 2024. https://doi.org/10.1109/JSEN.2023.3340717.
[11] Chun, Y. L., Ren, Y. H., Megan, T., & Yi, C. W., "Pulsed eddy current sensor for cascade electrical conductivity and thickness estimation in nonferrous metal plates," *IEEE Sensors Journal*, 23(8), 8323–8334, 2023. https://doi.org/10.1109/JSEN.2023.3257316.
[12] Ahmed, N., Moneer, A., Fahmi, S., Damhuji, R., Kharudin, A., & Al-Douri, Y., "Challenges in improving the performance of eddy current testing: Review," *Measurement and Control*, 52(1–2), 46–64, 2019. https://doi.org/10.1177/0020294018801382.
[13] Sear, J., "A novel variant of the H-U field formulation for magnetostatic and eddy current problems," *COMPEL - The International Journal for Computation and Mathematics in Electrical and Electronic Engineering*, 38(5), 1545–1561, 2019. https://doi.org/10.1108/COMPEL-12-2018-0536.
[14] Calvano, F., "Electromagnetic Non-Destructive Evaluation and Inverse Problems," Ph.D. dissertation, Dept. Elect. Eng., Univ. of Naples Federico II, Naples, Italy, 2010. https://doi.org/10.6092/UNINA/FEDOA/8375.
[15] Brown, M. L., "Calculation of 3-dimensional eddy currents at power frequencies," *Engineering Physics*, 129(1), 46–53, 1982. https://doi.org/10.1049/ip-a-1.1982.0007.
[16] Albanese, R., "Solution of three-dimensional eddy current problems by integral and differential methods," *IEEE Transactions on Magnetics*, 24(1), 98–101, 1988. https://doi.org/10.1109/20.43865.
[17] Biro, O., & Kurt, P., "On the Use of the Magnetic Vector Potential in the Finite Element Analysis of Three-Dimensional Eddy Currents," *IEEE Transactions on Magnetics*, 25(4), 3145–3159, 1989. https://doi.org/10.1109/20.34388.
[18] Zuo, M. H. M., & Teixeira, F. L., "Finite element analysis of electromagnetic boundary value problems with Galerkin formulation," *IEEE Transactions on Magnetics*, 31(6), 3483–3486, 1995. https://doi.org/10.1109/20.477828.
[19] Kovar, L. S., O'Rourke, R. W., & Morrow, M. J. S., "Galerkin finite element methods in the analysis of electromagnetic fields: Application to boundary condition modelling," *IEEE Transactions on Microwave Theory and Techniques*, 50(3), 739–748, 2002. https://doi.org/10.1109/22.987701.
[20] Abdelhak, A., Abderrahmane, A., Tarik, B., Bachir, A., & Amor, G., "Numerical simulation and experimental studies of rotational eddy current detection of cracks around rivet holes," *Studies in Engineering and Exact Sciences*, 5(2), e5964, 2024. https://doi.org/10.54021/seesv5n2-047.